

# Stability of a Self-Excited Machine Due to the Mechanical Coupling

M. Soltan Rezaee, M. R. Ghazavi, A. Najafi, W.-H. Liao

**Abstract**—Generally, different rods in shaft systems can be misaligned based on the mechanical system usages. These rods can be linked together via U-coupling easily. The system is self-stimulated and may cause instabilities due to the inherent behavior of the coupling. In this study, each rod includes an elastic shaft with an angular stiffness and structural damping. Moreover, the mass of shafts is considered via attached solid disks. The impact of the system architecture and shaft mass on the instability of such mechanism are studied. Stability charts are plotted via a method based on Floquet theory. Eventually, the unstable points have been found and analyzed in detail. The results show that stabilizing the driveline is feasible by changing the system characteristics which include shaft mass and architecture.

**Keywords**—Coupling, mechanical systems, oscillations, rotating shafts.

## I. INTRODUCTION

RECENTLY, vibration and stability of rotordynamics have been analyzed by many researchers experimentally, numerically and analytically [1]-[7]. Some of these investigations have concentrated on the behavior of mechanisms and couplings [8]-[12]. Asokanathan and Hwang [13] used the averaging method and obtained a closed-form function for dynamic instability zones related to combinational resonance. Asokanathan and Meehan [14] considered a two-Degree-of-freedom (two-DOF) nonlinear model. Mazzei [15] investigated the resonances of a U-joint driveline system. Bulut and Parlar [16] considered a two-DOF model. Their system consists of two torsionally elastic shafts connected through a Hooke's joint. They linearized the equations of motion (EOM) and stability of the solutions was analyzed numerically. Moreover, the connected shafts in the drive system of the rolling mill were studied by Shi et al. [17]. The effects caused by the U-joint angle and the impact on the dynamic stability of the rotary system were analyzed and the nonlinear torsional vibration model of the shaft system which includes parametric excitation was investigated. Then, Amer et al. [1] considered the torsional oscillations of a rolling mill like that had been studied by Shi et al. [17]. The vibration of

shaft system was controlled by using active control. The worst resonances were determined, and the steady state response of the driveline was investigated numerically. Ultimately, the behavior of a two-axis driveline system was analyzed by SoltanRezaee and Ghazavi [5]. It is necessary to note that in all of the mentioned papers, the inertia of shafts was ignored or modeled only with one disk.

There are a few researches on the torsional vibration of a shaft system which involves more than one rotary disk on each shaft. Alugongo [18] proposed a two-axis model for analyzing torsional vibration of a propeller shaft with a crack-induced excitation, by considering the elasticity and energy of the system. Jinli et al. [19], [20] considered the transmission system. The mathematical model was solved by the state space method and the effect of the joint angle on the vibration was obtained.

To the best knowledge of the authors, dynamic stability of a multi-body disk-shaft system connected through flexible joints has not been analyzed yet. The current powertrain system consists of two elastic shafts interconnected through a U-coupling. The influence of angle variations of the joint and inertia of system on the stability of a power train system are the main parameters which are analyzed in detail. Finally, stabilizing method by changing the system parameters is discussed.

## II. MODELING

Consider a powertrain system, including two shafts, which are driven through a mechanical coupling. The shafts include a flexible bar with a torsional stiffness and viscous damping coefficient of  $k_i$  and  $c_i$ , respectively. At both ends of each shaft, there is a disk with a rotary inertia of  $J_i$ . The driveline system can be driven by an electric motor or a mechanical drive with a constant angular velocity of  $\Omega_0$ . This system is with angular misalignment of  $\alpha$ .

The torsional EOM of the system can be obtained by a combinational technique. The driveline is considered as two separate parts (the driving as well as the driven shaft) with double disk at the ends of each shaft. The equations of torsional motion for rotational dynamics of each rigid disk by using the Newton's Law can be derived as follows

$$J_1 \ddot{\phi}_1 = c_1 (\dot{\phi}_2 - \dot{\phi}_1) + k_1 (\phi_2 - \phi_1) - M_1, \quad (1)$$

$$J_2 \ddot{\phi}_2 = -c_1 (\dot{\phi}_2 - \dot{\phi}_1) - k_1 (\phi_2 - \phi_1) + M_2, \quad (2)$$

M. Soltan Rezaee is with Department of Mechanical Engineering, Tarbiat Modares University, Tehran, Iran (e-mail: soltanrezaee@gmail.com).

M. R. Ghazavi is with Department of Mechanical Engineering, Tarbiat Modares University, Nasr Bridge, Tehran, Iran (corresponding author, telefax: +9821-8288-3362; e-mail: ghazavim@modares.ac.ir).

A. Najafi is with Mechanical Rotary Equipment Department, Niroo Research Institute, Tehran, Iran (e-mail: anajafi@nri.ac.ir).

W.-H. Liao is with Department of Mechanical and Automation Engineering, The Chinese University of Hong Kong, Hong Kong, China (e-mail: whliao@cuhk.edu.hk)

$$J_3 \ddot{\varphi}_3 = c_2 (\dot{\varphi}_4 - \dot{\varphi}_3) + k_2 (\varphi_4 - \varphi_3) - M_3, \quad (3)$$

$$J_4 \ddot{\varphi}_4 = -c_2 (\dot{\varphi}_4 - \dot{\varphi}_3) - k_2 (\varphi_4 - \varphi_3) + M_4, \quad (4)$$

In the following, the relation between input and output angular velocity and the transferred torque of the joint is stated as [21]

$$\begin{aligned} \sigma &= \frac{\dot{\varphi}_3}{\dot{\varphi}_2} = \frac{M_2}{M_3} \\ \rightarrow \sigma &= \frac{\cos \alpha}{1 - \sin^2 \alpha \sin^2 \varphi_2}, \end{aligned} \quad (5)$$

Herein, the derivations of angular positions of disks ( $\varphi$ ) and their relations with torsional coordinates ( $\theta$ ) can be computed as

$$\dot{\varphi}_1 = \Omega_0 \rightarrow \ddot{\varphi}_1 = 0, \quad (6)$$

$$\varphi_2 = \varphi_1 + \theta_1 \rightarrow \dot{\varphi}_2 = \dot{\varphi}_1 + \dot{\theta}_1 \rightarrow \ddot{\varphi}_2 = \ddot{\theta}_1, \quad (7)$$

$$\dot{\varphi}_3 = \sigma (\Omega_0 + \dot{\theta}_1) \rightarrow \ddot{\varphi}_3 = \dot{\sigma} (\Omega_0 + \dot{\theta}_1) + \sigma \ddot{\theta}_1, \quad (8)$$

$$\varphi_4 = \varphi_3 + \theta_2 \rightarrow \dot{\varphi}_4 = \dot{\varphi}_3 + \dot{\theta}_2 \rightarrow \ddot{\varphi}_4 = \ddot{\varphi}_3 + \ddot{\theta}_2, \quad (9)$$

Finally, (10) and (11) are the torsional EOM of the multi-body two-DOF system model.

$$\begin{aligned} 0 &= J_2 \ddot{\theta}_1 + c_1 \dot{\theta}_1 + k_1 \theta_1 \\ &+ \sigma \left( J_3 (\dot{\sigma} (\Omega_0 + \dot{\theta}_1) + \sigma \ddot{\theta}_1) - c_2 \dot{\theta}_2 - k_2 \theta_2 \right), \end{aligned} \quad (10)$$

$$M_4 = J_4 (\dot{\sigma} (\Omega_0 + \dot{\theta}_1) + \sigma \ddot{\theta}_1 + \ddot{\theta}_2) + c_2 \dot{\theta}_2 + k_2 \theta_2. \quad (11)$$

Equations (10) and (11) represent non-linear equations for oscillation of powertrain system. These equations can be linearized via McLaurin series and neglecting the nonlinear higher order terms under the assumptions of small oscillation amplitudes and frequencies.

The approximation of the transfer ratio of a Cardan coupling, by the first two terms of McLaurin series can be stated as

$$\sigma \approx \sigma \Big|_{\theta_1=0} + \frac{\partial \sigma}{\partial \theta_1} \Big|_{\theta_1=0} \theta_1 = \varepsilon + \frac{\partial \sigma}{\partial \varphi_2} \Big|_{\theta_1=0} \theta_1 = \varepsilon + \frac{\dot{\varepsilon} \theta_1}{\Omega_0}, \quad (12)$$

where

$$\begin{aligned} \varepsilon &= \frac{\cos \alpha}{1 - \sin^2 \alpha \sin^2 \tau}; \\ \tau &= \Omega_0 t, \end{aligned} \quad (13)$$

where  $\tau$  is the dimensionless time and

$$\begin{aligned} \dot{\sigma}(\theta_1) &= \frac{\partial \sigma}{\partial \varphi_2} \dot{\varphi}_2 \approx \left( \frac{\partial \sigma}{\partial \varphi_2} \Big|_{\theta_1=0} + \frac{\partial}{\partial \varphi_2} \left( \frac{\partial \sigma}{\partial \varphi_2} \Big|_{\theta_1=0} \theta_2 \right) \right) (\Omega_0 + \dot{\theta}_1) \\ &\approx \dot{\varepsilon} + \frac{\dot{\varepsilon} \dot{\theta}_1}{\Omega_0} + \frac{\ddot{\varepsilon} \theta_1}{\Omega_0}, \end{aligned} \quad (14)$$

The matrix-vector form of the presented system model can be written as

$$\begin{aligned} \begin{bmatrix} J_2 + J_3 \varepsilon_1^2 & 0 \\ J_4 \varepsilon_1 & J_4 \end{bmatrix} \begin{Bmatrix} \ddot{\theta}_1 \\ \ddot{\theta}_2 \end{Bmatrix} + \begin{bmatrix} c_1 + J_3 \varepsilon_1 \dot{\varepsilon}_1 & -c_2 \varepsilon_1 \\ 2J_4 \dot{\varepsilon}_1 & c_2 \end{bmatrix} \begin{Bmatrix} \dot{\theta}_1 \\ \dot{\theta}_2 \end{Bmatrix} \\ + \begin{bmatrix} k_1 + J_3 (\varepsilon_1 \ddot{\varepsilon}_1 + \dot{\varepsilon}_1^2) & -k_2 \varepsilon_1 \\ J_4 \ddot{\varepsilon}_1 & k_2 \end{bmatrix} \begin{Bmatrix} \theta_1 \\ \theta_2 \end{Bmatrix} &= \begin{Bmatrix} -\Omega_0 J_3 \varepsilon_1 \dot{\varepsilon}_1 \\ M_4 - \Omega_0 J_4 \dot{\varepsilon}_1 \end{Bmatrix}. \end{aligned} \quad (15)$$

It is more convenient to write the governing equation in dimensionless form. To this end, the torsional coordinate's derivatives with respect to non-dimensional time are recomputed and the following dimensionless parameters are introduced:

$$\dot{\theta}_i = \frac{d}{dt} \theta_i = \frac{d}{d\tau} \theta_i \frac{d\tau}{dt} = \theta_i' \Omega_0 \rightarrow \ddot{\theta}_i = \theta_i'' \Omega_0^2; i=1,2. \quad (16)$$

$$\begin{aligned} \gamma &= \frac{J_4}{J_2}, \mu = \frac{J_3}{J_2}, \chi = \frac{c_2}{c_1}, \\ \kappa &= \frac{k_2}{k_1}, \xi = \frac{c_1}{2\sqrt{k_1 J_2}}, \Omega = \Omega_0 \sqrt{\frac{J_2}{k_1}}, \end{aligned} \quad (17)$$

where  $\xi$  and  $\Omega$  are the non-dimensional terms of damping ratio and angular velocity, respectively.

Finally, the EOM for torsional oscillation of powertrain system model (15) with respect to (16) and (17) can now be non-dimensionalized as

$$\begin{aligned} M\theta'' + C\theta' + K\theta = N &\rightarrow \begin{bmatrix} 1 + \mu \varepsilon^2 & 0 \\ \varepsilon & 1 \end{bmatrix} \begin{Bmatrix} \theta_1'' \\ \theta_2'' \end{Bmatrix} \\ + \begin{bmatrix} \frac{2\xi}{\Omega} + \mu \varepsilon \varepsilon' & -\frac{2\xi \chi \varepsilon}{\Omega} \\ 2\varepsilon' & \frac{2\xi \chi}{\Omega \gamma} \end{bmatrix} \begin{Bmatrix} \theta_1' \\ \theta_2' \end{Bmatrix} + \begin{bmatrix} \frac{1}{\Omega^2} + \mu (\varepsilon'' \varepsilon + \varepsilon'^2) & -\frac{\kappa \varepsilon}{\Omega^2} \\ \varepsilon'' & \frac{\kappa}{\Omega^2 \gamma} \end{bmatrix} \begin{Bmatrix} \theta_1 \\ \theta_2 \end{Bmatrix} \\ = - \begin{Bmatrix} \mu \varepsilon \varepsilon' \\ \varepsilon' + \bar{M} \end{Bmatrix}. \end{aligned} \quad (18)$$

### III. ANALYSIS

Equation (18) is for the governing equations of torsional motion for the two-DOF model, which has periodically varying coefficients. As shown, there is a set of linear OD equations.

A state–space display of homogeneous part of (18) can be given as.

$$\begin{Bmatrix} \theta_1' & \theta_2' & \theta_1'' & \theta_2'' \end{Bmatrix}^T = \begin{bmatrix} \mathbf{0}_{2 \times 2} & \mathbf{I}_{2 \times 2} \\ -\mathbf{K}/M & -\mathbf{C}/M \end{bmatrix} \begin{Bmatrix} \theta_1 & \theta_2 & \theta_1' & \theta_2' \end{Bmatrix}^T, \quad (19)$$

In this work, dynamic stability zones are investigated by means of a numerical method that is called monodromy matrix [22]. It determines the stability areas and resonance conditions of a system with parametric excitation. The instability occurs whenever the associated eigenvalues of the system have a positive real part in a parameter space. The obtained outputs are charts, which contain some of the most important system characteristics.

It is clear that the location of instability regions (resonance areas) on the figures depends on the natural frequencies of system. The  $k$ -th order harmonic and sub-harmonic resonance zones related to the  $i$ -th vibration mode as well as the difference and sum type combinational resonance zones are given by

$$\begin{aligned} \Omega_{H,ik} &= \frac{\omega_i}{2k}, \Omega_{S,ik} = \frac{\omega_i}{2k-1}, \\ \Omega_{CS,12k} &= \frac{\omega_2 + \omega_1}{2k}, \Omega_{CD,12k} = \frac{\omega_2 - \omega_1}{2k}; \end{aligned} \quad (20)$$

$i = 1, 2; k = 1, 2, 3, \dots$

IV. RESULTS AND DISCUSSIONS

As shown in Fig. 1, the diagram peaks show the natural frequencies of multi-body system.

On the other hand, the first and second order harmonic, sub-harmonic, difference and sum combinational resonance zones related to the fundamental vibration modes of driveline are reported in Table I.

TABLE I  
THE HARMONIC  $\Omega_H$ , SUB-HARMONIC  $\Omega_S$ , SUM COMBINATIONAL  $\Omega_{CS}$  AND DIFFERENCE COMBINATIONAL  $\Omega_{CD}$  PARAMETRIC RESONANCES OF THE SHAFT SYSTEM

Resonance	First mode	Second mode
$\Omega_{H,1}$	0.270	0.135
$\Omega_{H,2}$	0.655	0.328
$\Omega_{S,1}$	0.540	0.180
$\Omega_{S,2}$	1.310	0.437
$\Omega_{CS,12}$	0.925	0.463
$\Omega_{CD,12}$	0.385	0.193

The analysis of dynamic stability is done via the monodromy matrix method based on the assumptions that the natural frequencies in Fig. 1 were achieved. Fig. 2 illustrates the results of stability analysis where the colored points (shaded zone) show the unstable areas. The vertical axis

displays the coupling angle, and the horizontal axis depicts the non-dimensional angular velocity. It should be noted that the characteristics of the considered shafts are taken identical and the damping ratio is equal to 0.0003 in the following case studies.

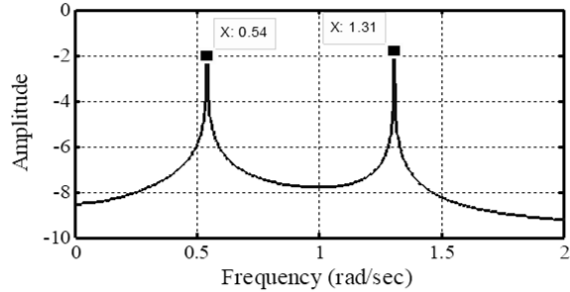


Fig. 1 The frequency response shown by means of fast Fourier transform (FFT) algorithm

The location of unstable points on the diagram depends on the natural frequencies of model. The peaks of colored areas on the horizontal axis are equal to the computed points on Table I. Certain instability regions, which are previously calculated analytically, are labeled. This was achieved in order to provide an idea about the various types of dynamic instabilities in the assumed parameter space. A perusal of Fig. 2 demonstrates that the location of the analytical results as reported in Table I, are in agreement with the peaks of the numerical ones. As a result, a more accurate investigation, which illustrates the impact of other modes, may be performed.

Generally, by increasing the angle from zero (where no excitation exists), the unstable zones extend and become wider. It is seen that different types of instability regions are revealed, but combinational resonances. The resonances, which are associated with the lower oscillation mode, have more clarity.

Usually, the peaks depending on higher system natural frequencies occur in high misalignment (e.g.  $\Omega_{H,22}$  and  $\Omega_{S,22}$ ). Furthermore, by increasing the angle of misalignment (the angle between intersecting shaft axes), some new unstable areas emerge that are not generally important for practical applications.

Determination of factors that affect the dynamic stability of powertrain is necessary. To this end, several cases are evaluated. One of the most remarkable factors is the system geometry. The system geometry includes the Hooke’s angle (the angle between two yokes of coupling). Often in practice, these angles are considered to be less than 1 rad in disk-shaft mechanisms and the impact of geometry in this range is evaluated.

The inertia of driveline is another factor that affects the stability and can be checked. The rigid disks represent the pulley or gear that may be attached to the shaft or addressed the rotary inertia of model. The results are charts which include a pair of the present model parameters and show the system stability. In all of these cases, the stability is verified

point by point.

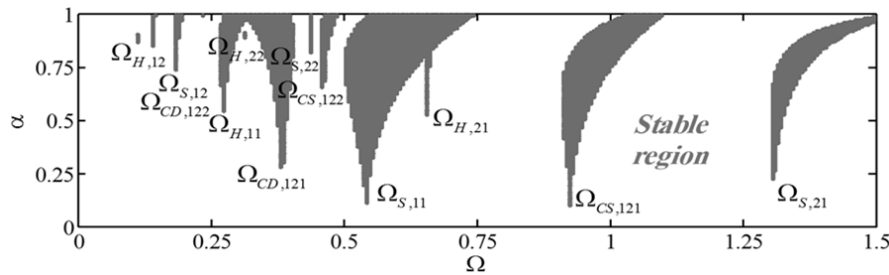


Fig. 2 Stability chart: investigation of the obtained results for unstable points

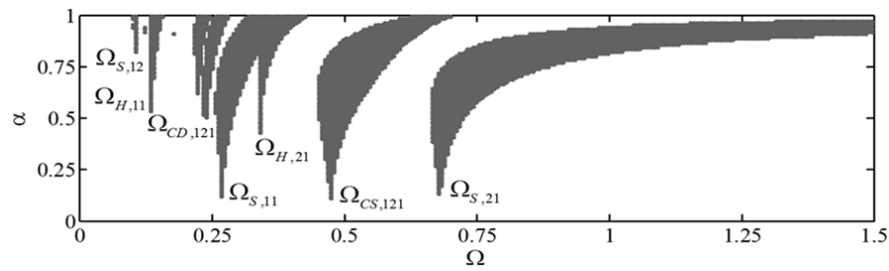


Fig. 3 Stability chart: effect of driven shaft inertia ( $\mu=5$  and  $\gamma=5$ )

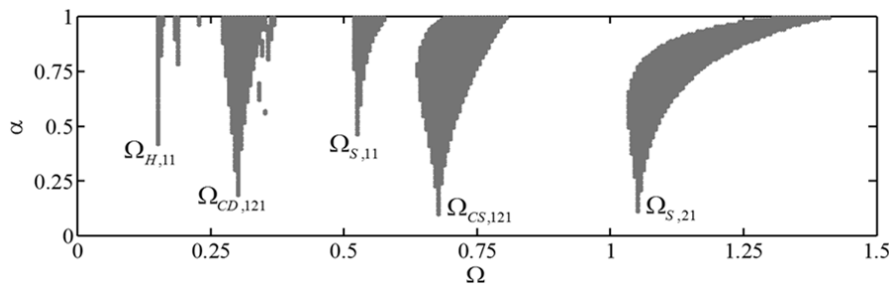


Fig. 4 Stability diagram: effect of final disk inertia ( $\mu=1$  and  $\gamma=5$ )

In order to evaluate the effect of the system inertia moment, two amounts are considered for the driven disk-shaft. To depict the inertia impact of multi-body system, the inertia of the second shaft is five times greater than the first one (Fig. 3). By comparison between Figs. 4 and 3, it can be observed that as driven shafts inertia increase, the peaks shift toward a lower velocity that should be considered in designing. By analyzing graphs, it can be deduced that increasing the system inertia has a significant stabilizing effect. In addition, many unstable regions are close together or merged, so that they are not explicitly recognizable.

Now, the inertia effect of the fourth disk, which is on the end of the driven shaft (the output segment of the multi-body system) is investigated (Fig. 4) in a system with some specified parametric values ( $\mu=1$  and  $\gamma=5$ ). It can be concluded from comparing Fig. 4 with 3, that by changing the disk inertia, the peak position varies. Consequently, the natural frequencies of the powertrain system decrease when inertia ratio increases. This is more pronounced, particularly at low velocity which converts the system to an unreliable one. By

comparison between Figs. 3 and 4, it is clear that the effects of driven shaft inertia are different than that of the final disk, quantitatively. The reason is that unstable zones have considerably changed. Therefore, the dynamic behavior and parametric instabilities of the driveline system are not certain and exactly predictable, in some cases. This fact demonstrates the significance of quantitative analysis.

## V. CONCLUSION

In this study, the behavior of a driveline is considered, and stability circumstances are analyzed. The shaft system includes two rotating rods interconnected through U-coupling. The EOM consist ODE, which is evaluated numerically. The mass of each shaft is considered via solid disks. The impacts of the architecture, the input speed and the shaft mass are studied. The outputs have been studies in the instability charts and examined in detail. Finally, the obtained results are as follows:

Modeling of rotating rod mass causes more accurate results, which is considerable for studying the shaft systems.

Consequently, the modeling is suitable for oscillations identification of drivelines used in various mechanisms and systems.

Enhancing the mass of second rod causes to obtain narrower unstable areas. Additionally, the variation of this character leads to the change in the torsional fundamental frequencies in mechanical systems.

## REFERENCES

- [1] F. Vesali, M. A. Rezvani, M. Kashfi, Dynamics of universal joints, its failures and some propositions for practically improving its performance and life expectancy, *Journal of Mechanical Science and Technology*, 26 (2012) 2439-2449.
- [2] M. SoltanRezaee, M. Afrashi, S. Rahmanian, Vibration analysis of thermoelastic nano-wires under Coulomb and dispersion forces, *International Journal of Mechanical Sciences*, 53(5) (2018) 33-43.
- [3] M. SoltanRezaee, M. R. Ghazavi, Thermal, size and surface effects on the nonlinear pull-in of small-scale piezoelectric actuators, *Smart Materials and Structures*, 142-143 (2018) 095023.
- [4] M. SoltanRezaee, M. R. Ghazavi, A. Najafi, Parametric resonances for torsional vibration of excited rotating machineries with nonconstant velocity joints, *Journal of Vibration and Control*, 24(15) (2018) 3262-3277.
- [5] M. SoltanRezaee, M.-R. Ghazavi, Obtaining Stable Cardan Angles in Rotating Systems and Investigating the Effective Parameters on System Stability (in Persian), *Journal of Modares Mechanical Engineering*, 14 (2015) 163-170.
- [6] M. SoltanRezaee, M. R. Ghazavi, A. Najafi, S. Rahmanian, Stability of a multi-body driveshaft system excited through U-joints, *Meccanica*, 53(5) (2018) 1167-1183.
- [7] M. SoltanRezaee, M. R. Ghazavi, A. Najafi, Mathematical modelling for vibration evaluation of powertrain systems, *Proceedings of the IASTED International Conference on Modelling, simulation and identification (MSI 2017)*, Calgary, Canada, July 19-20 (2017) 73-79.
- [8] M. SoltanRezaee, M.R. Ghazavi, A. Najafi, Dynamic Stability of a System Including Three Shafts, *Proceedings of Second International Conference on Advances in Robotic, Mechanical Engineering and Design (ARMED 2012)*, Dubai, UAE, September, 20-21 (2012).
- [9] G. Bulut, Dynamic stability analysis of torsional vibrations of a shaft system connected by a Hooke's joint through a continuous system model, *Journal of Sound and Vibration*, 333 (2014) 3691-3701.
- [10] G. Yan, Analysis and optimization of torque variation in steering column assembly, in: *Proceedings of the FISITA 2012 World Automotive Congress*, Springer, 2013, pp. 57-67.
- [11] C. Peressini, A. Guzzomi, D. Hesterman, Torsional receptances and variable inertia of a two-inertia model of a universal joint, in: *New Trends in Mechanism and Machine Science*, Springer, 2013, pp. 577-585.
- [12] D. R. Johnson, K. Wang, Analysis of a Flexibly Mounted Shaft Incorporating a Non-Constant Velocity Coupling With Dynamic Misalignment, in: *ASME 2011 International Design Engineering Technical Conferences and Computers and Information in Engineering Conference*, American Society of Mechanical Engineers, 2011, pp. 1023-1032.
- [13] S. Asokanathan, M.-C. Hwang, Torsional instabilities in a system incorporating a Hooke's joint, *Journal of Vibration and Acoustics*, 118 (1996) 368-374.
- [14] S. Asokanathan, P. Meehan, Non-linear vibration of a torsional system driven by a Hooke's joint, *Journal of Sound and Vibration*, 233 (2000) 297-310.
- [15] A. Mazzei, Passage through resonance in a universal joint driveline system, *Journal of Vibration and Control*, 17 (2010) 667-677.
- [16] G. Bulut, Z. Parlar, Dynamic stability of a shaft system connected through a Hooke's joint, *Mechanism and Machine Theory*, 46 (2011) 1689-1695.
- [17] P. Shi, J.-z. Li, J.-s. Jiang, L. Bin, D.-y. Han, Nonlinear dynamics of torsional vibration for rolling mill's main drive system under parametric excitation, *Journal of Iron and Steel Research, International*, 20 (2013) 7-12.
- [18] A. Alugongo, Parametric excitation and wavelet transform analysis of ground vehicle propeller shaft, *Journal of Vibration and Control*, 20 (2012) 280-289.
- [19] X. Jinli, S. Xingyi, P. Bo, Numerical analysis and demonstration: Transmission shaft influence on meshing vibration in driving and driven gears, *Shock and Vibration*, 501 (2015) 365084.
- [20] X. Jinli, W. Lei, L. Wenxin, Influence of Bearing Stiffness on the Nonlinear Dynamics of a Shaft-Final Drive System, *Shock and Vibration*, 2016 (2016).
- [21] H.-C. Seherr-Thoss, F. Schmelz, E. Aucktor, *Universal joints and driveshafts: analysis, design, applications*, Springer Science & Business Media, Berlin, Germany., 2006.
- [22] L. Meirovitch, *Methods of analytical dynamics*, McGraw-Hill, New York, USA., 1970.